ATLAS Internal Note
PHYS/MUON-No XXX
July, 30th 2003

Influence of the alignment of the muon chambers to SM Higgs reconstruction H→4 μ

D. Fassouliotis, C. Kourkoumelis, S. Stefanidis
University of Athens

D. Levin
University of Michigan

Abstract

A GEANT3 based Monte Carlo simulation has been used to estimate the effect of end-cap misalignments relative to the barrel Muon Spectrometer on the reconstruction of the SM Higgs. A constrained fit algorithm using a Breit-Weigner Z mass distribution was implemented and its effect on the Higgs mass reconstruction resolution evaluated. In addition, a study of the misalignment was performed using the Z → μμ decay channel.

1. INTRODUCTION

We report on a study of the muon spectrometer alignment and its impact on reconstruction of the Higgs particle decay to four muons. The results show how the width of the Higgs and the discovery capabilities are influenced by possible misalignments of the muon system. A method of increasing the resolution in the reconstruction of the Higgs particle, by constraining the Z-mass is also presented.

In general the momentum determination of high energy muons will be done combining the information of the inner detector with that coming from the muon spectrometer. In this study we concentrate exclusively on the muon system. In a follow-up note the information of the inner detector will be combined and the sensitivity to the MSSM Higgs decay to two muons will also be evaluated.

The muon alignment within the barrel and within the end-caps (EC) (Ref 1) is designed to be well controlled (within tens of microns) using the praxial and projective alignment platforms (barrel) and the alignment bars (EC). These optical systems are designed to reduce the systematic error in the track reconstruction due to temperature or stress induced by spatial displacements of the chambers. Furthermore, their accuracy and calibration can be evaluated and controlled using cosmic rays and dedicated toroid magnet-off straight-track runs ensuring an alignment within tolerances of the barrel and the EC independently. However the relative alignment of the barrel with respect to the EC lacks direct optical links and may have large uncertainties. We therefore, studied this situation in order to determine the maximum misalignment size, which could be tolerated without substantial loss in the Higgs discovery potential. At the same time we tried to determine the minimum misalignment to which the Z mass reconstruction could be sensitive.

2. ANALYSIS

2.1 Event Generation / Simulation

For the simulation of Higgs events used in this study, the PYTHIA (6.203) event generator was used. A GEANT3 based Monte Carlo program, LHCTOR -version 40900- (Ref 2) was invoked to model the muon system. This program includes an internal passive mass to approximate the energy loss in the internal detectors. In the event generation, only the specific channel Higgs to four muons was turned on. For this analysis we generated two Higgs masses 200 and 300 GeV/c^2, with widths 1.36 GeV/c^2 and 8.36 GeV/c^2 respectively. The widths which we evaluated after PYTHIA‘s muon inner Bremstrahlung (FSR) and a BW fit in the same mass interval as the reconstructed data mentioned below, were 2.7 GeV/c^2 and 10.9 GeV/c^2 respectively. The muon hits were reconstructed using MUONBOX (version 60305) (Ref 3), which produced an ntuple with the reconstructed track parameters for further analysis. In the MUONBOX reconstruction an 85 μm average intrinsic tube resolution, a multilayer alignment error of 20 μm and a chamber alignment error 30 μm.(within the same tower) were used. In order to focus singularly on alignment effects and to speed processing time, no random noise hits were generated. Final results may be slightly influenced by this choice. For each mass value, about 5,000 events were generated. Table 1 shows the relative acceptances after the $p>5$ GeV/c and $p_t>3$ GeV/c cuts were applied to the four final state muons, together with the trigger cut (one muon with $p_t>20$ GeV/c and $|\eta|<2.5$). In the GEANT detector

simulation delta ray production was enabled and particles were followed down to a cutoff of 10 MeV.

2.2 Event Selection and Reconstruction

At reconstruction level we required four "good" muon candidates, two positive and two negative ones in a pseudorapidity interval $|\eta|<2.5$. As a first step in the analysis, we added back the energy which the muons lost while traversing the material of the inner detectors (mainly in the hadronic calorimeter). A parameterization of the energy loss as a function of the muon momentum and pseudorapidity was obtained from the MuonIdentification package (Ref 4). In Figure 1 we compare the parameterization with the actual loss from the Monte Carlo generation for muons of an average momentum of 50 GeV/c.

After this energy loss correction the reconstructed opposite sign di-muon masses were required to be within 18 GeV/c^2 from the nominal Z mass. The selection of the pairing among the two possible combinations is performed during the constrained fit procedure and is described below. Finally, for an event to be counted as a Higgs candidate we apply a mass window cut based on the Higgs invariant mass distribution. This, as explained below, is set in all cases to 1.5 times the original (without misalignment) Breit-Wigner width, evaluated for the reconstructed and the fitted case respectively. In table 1, the efficiency at different steps of the analysis is shown.

	Higgs 200	**Higgs 300**
Generated	5000 events	5000 events
	Accepted %	
4 μ's simulated	89.0	91.0
4 μ's within acceptance	76.6	78.3
4 μ's reconstructed	72.9	74.4
Z's within 18 GeV/c^2	60.2	62.4
H's in 1.5 BW width	54.8	55.2

Table 1: Percentage of accepted Higgs events at each step of the analysis

2.3 Mass constrainted fit

In order to improve the resolution of the reconstructed Higgs candidates we took in advantage the fact that each of the two di-muon effective masses should be compatible with the Z mass (for the cases where $m_H > 160$ GeV/c^2). For this purpose, we developed a program, both in Fortran and OO C++, which takes the four-vector momentum of each muon in the corresponding di-muon pair and changes them in order to minimize the χ^2 of the kinematical quantities namely:

$$\{(\Delta p/\sigma p)^2 + (\Delta\theta/\sigma\theta)^2 + (\Delta\varphi/\sigma\varphi)^2\}$$

under the constraint of a fixed di-muon mass. Quantities with Δ_i correspond to the difference between the starting and the fitted values, while σ_i correspond to the error on the specific kinematical quantity.

After several tries we decided to use the errors originating from the Track Fit matrix. The existence of non-gaussian tails in the track fit presents problems that cannot be solved by the constrained fit since it is not possible to distinguish between a well reconstructed muon and a badly reconstructed one if they have errors of similar size. We were thus unable to establish a correlation between the physical quantities (e.g. $\chi 2$ of the track fit, number of associated hits, etc.) and the badly reconstructed tracks.

If indeed the starting value of the reconstructed invariant mass is close to the nominal value, then the Higgs mass resolution can be improved if we constrain the two dimuon pairs to the nominal Z mass. On the other hand, events which are produced with invariant masses far from the nominal Z mass are artificially forced to be reconstructed with a far away value, thus deteriorating the Higgs mass resolution. As a matter of fact, fixing the di-muon mass to the nominal Z mass, fixes the mean value of the Higgs mass distribution but does not improve the resolution in any significant way. We, therefore, decided to follow a non-fixed mass constraint strategy allowing the mass constraint to vary following a Breit-Wigner distribution according to the Z parameters.

2.4 Strategy for defining the spectrum of masses where the constrained fit was be performed

As a starting point for the mass constraint, the reconstructed di-muon mass was used. If the mass was outside a certain window (e.g. ± 20 GeV/c^2 from the nominal Z-mass) no fit was performed. Otherwise, a scan was performed in the direction towards the nominal Z mass using initially a large step size (e.g. 0.5 GeV/c^2) followed by a finer one (e.g. 0.125 GeV/c^2), as one approached the nominal Z-mass. We defined a net probability as the product of the χ^2 probability of the fit and the probability of having the specific mass in a Breit-Winger distribution centered at the nominal Z mass value and within the nominal[1] width. If the probability corresponding to three successive steps became continuously smaller, then the loop was stopped and the chosen mass- where the fit was based- was the one with the higher probability. This procedure was repeated for the second di-muon effective mass. A combined probability was then formed for the whole two di-muon combination and the pairing was chosen according to this over all probability. Table 2 shows the percentage of failures of the above pairing criteria for two different Higgs masses

Higgs mass (GeV/c^2)	Misses
200	133/3185 = (4 ± 0.3)%
300	62/3047 = (2 ± 0.2)%

Table 2: Percentage of events where the wrong muon pairing was selected..

Figures 2a and 2b, show the total probability and the $\chi 2$ probability respectively as a function of the di-muon mass for a typical event. A green arrow indicates the unfit mass value and the red arrow the mass value chosen after the fit.

Figure 3 shows the reconstructed minus generated di-muon mass from 200 GeV/c^2 Higgs decays, before and after the constrained fit. Figure 4 shows the

[1] The width does not necessarily have to be the nominal one, since part of this information is already included in the reconstruction spectrum.

reconstructed minus the generated Higgs mass before and after the constrained fit for a 200 GeV/c^2 Higgs. Figure 5 shows the same as Figure 4 but for a 300 GeV/c^2 Higgs. In the last three plots we show the reconstructed minus the generated mass values in order to subtract the intrinsic Higgs width. The widths shown in these plots are due to the experimental resolution only.

The constraint fit corrects principally the absolute value of the momentum. The energy loss correction is successfully done (agrees with the MC energy loss) and the direction of track is left almost unchanged

The improvement of Higgs width (Γ) is:

~ 20 % for the 200 GeV/c^2 Higgs

~ 13 % for the 300 GeV/c^2 Higgs,

which means, that in actual life the signal/background ratio for the Higgs search will be improved significantly by performing the constraint fit using the information from the muon spectrometer reconstruction alone. For a 200 GeV/c^2 Higgs in particular, due to the low intrinsic width, the improvement in the reconstruction is reflected directly in the S/B ratio.

3. ALIGNMENT STUDIES

As discussed above, our primary objective is to understand the effect of misalignments of EC with respect to the barrel. Misalignment studies were performed by introducing the corresponding translation or rotation in the MDT geometrical data base and then reconstructing tracks with this altered database. The hits which form the track are originally generated with the original database in which all chambers are ideally positioned. The alternative way to study this effect (a study which eventually has to be carried out in order to determine precisely the misalignment) is to consider high energy tracks passing from both the barrel and end-cap chambers. .

Two kinds of translations and rotations have been studied. The global translations are made with respect to an axis along the beams (named in the following as Z translation) and with respect to a transverse axis (in this case the ATLAS x axis, named as T translation). Following the same philosophy, a set of rotations around the z axis and another one around the x- ATLAS axis were performed. As far as the rotations around the x-axis are concerned, **each** EC sector (EI, EM and EO) was rotated by the same angle, around axes which were parallel to each other but their center was located at the z-position of the corresponding sector Both the translations and the rotations were applied for only one of the two ECs while the other was left in its original position and used for reference. The translations performed were 1, 3 and 5 mm, while the rotations 2.5, 5 and 10 mrad. Large values were chosen in order to have a noticeable result with moderate MC statistics. Interpolation/extrapolation of the values obtained this way, can be used to estimate the effect of other misalignment values.

Furthermore, two more types of translations were performed in order to compare with previous studies (Ref 5) and verify them using significantly more statistics. Both concerned the projective alignment and displaced all the middle stations of the muon spectrometer. In the first case they were translated randomly and in the second in such a way to have everywhere similar shifts in the momenta of positive and negative muons respectively. The shifts performed were 100, 200 and 300 μm. The random case, in agreement with the previous study, showed no significant effect on the detector performance and therefore was not treated further. The systematic misalignment case had, as expected, a more important impact and it

was further analyzed in order to be used as a reference. From the three possible translations in the chamber rest frames (Ref 6), the S ones (parallel to the MDT axis) affect much less the reconstruction and therefore we concentrate on the z translations for this study.

3.1 Effect of misalignments on the Reconstructed Higgs mass

According to the size and the type of the misalignment induced, an increase of the width of the reconstructed Higgs mass was observed. As expected, no significant change in the mean value of the distribution was observed (see figs 6 and 7), since the effect of the misalignment does not influence in the same way all tracks. Both in the case of the directly reconstructed Higgs (a), as well as in the case of using a BW Z mass constraint (b), the effect is approximately the same. In the case of a fixed Z mass constraint (not shown in the plots) the effect appeared to be significantly lower, at the price, however, of a poorer resolution in the Higgs mass, as discussed above.

The observed increase of the width is, however, not reflected to an equivalent loss in the number of the corresponding Higgs candidates, provided that a reasonable mass window is chosen. In this study we used a mass window of 1.5 Breit-Wigner[2] width (very close to two gaussian sigmas). As seen from Figures 6 and 7 and quantified in the following plots- outside this mass window, mainly lay events with one or more muons belonging to the non gaussian tails of the track reconstruction. The misalignments do not affect so dramatically the momentum resolution and therefore the number of events that "escape" the mass window shows a small increase.

In Figure 8, the increase of the width of the reconstructed Higgs mass is shown as a function of the size of the translation (a) or rotation (b) used. The lines are linear fits showing the trend of the increase. In Figure 9 the relative decrease of the accepted Higgs candidates in the selected mass window is shown as a function of the size of the translation (a), or rotation (b) used. It can be easily deduced that the slopes of the decrease of the event-count are much lower than the corresponding slopes of the increase of the width with one exception. As observed in Figure 9b the acceptance of the Higgs events drops significantly for large rotations about axes perpendicular to the beam. This decrease is not an effect of a large deterioration of the mass resolution, but stems from the fact that the muon reconstruction efficiency decreases rapidly. With a 10 mrad rotation (5 mrad), the single muon reconstruction efficiency in the whole EC drops to 89% (96%). This in turns results to a drop of the overall Higgs event acceptance to 82% (90% for 5 mrad). It should be noted that a 10 mrad rotation, which as a consequence moves the outer layer chambers by approximately 10 cm, is unrealistic and introduced only for the sake of interpolation to smaller rotations. However, this exercise points out, that rotations transverse to the beam should be well under control. The same trends appear also for a 300 GeV/c^2 Higgs as shown in Figure 10.

In the case of the systematic middle station misalignment, the reconstructed width increases “dramatically” while the accepted number of events drops very slowly, as shown in fig. 11. It must be stated here - as well as in the previous case- that the projective misalignments, introduced in this study, are by far above the

[2] We used a Breit-Wigner fit instead of a Gaussian one because it depends less on the interval used in the fit, providing thus a more reliable tool for the comparisons performed in this study.

accuracy allowed by the alignment system and were used only to allow us to observe the effect with the present statistics and be able to interpolate to smaller displacements.

3.2 Effect of misalignments on the Reconstructed Z mass

Possibly the only way to fully investigate and control the EC misalignments with respect to the barrel muon detector is to study the residuals of tracks crossing both areas. In this section we try to show that these types of misalignments manifest themselves quite clearly in the reconstructed Z mass distribution, even with a moderate number of recorded Z's. As can be inferred from Figure 12, where we plot the Z mass spectrum when at least one of the two muons was detected in the rotated EC, the effect of this rotation can be quite significant. In Figure 13, the increase of the width of the reconstructed Z mass is shown as a function of the size of the translation (a) or rotation (b) used. The lines are linear fits showing the trend of the increase. In these plots at least one muon of the Z decay products is required to be recorded in the misaligned EC, in the pseudorapidity intervals $1.0 < y < 1.5$, which is in the barrel-EC transition region, and $1.5 < y < 2.5$, which is in the forward EC region. As a reference the case where both muons are reconstructed in the barrel is also shown.

As it can be observed from the plots, the two different types of translation cause different change in the reconstructed Z mass width in different pseudorapidity intervals of the detector. The T type translations affect both muons in the transition and in the very forward region in the same way, resulting in similar slopes of the Z width increase, as a function of the displacement. On the contrary, the z-type translations affect the muons in the transition region more than the very forward ones, resulting in significant broadening of the Z width in the case where a muon is reconstructed in the pseudorapidity interval between 1.0 and 1.5. This is according to our expectations for this particular type of rotations. The edge of each EC sector is displaced most, resulting in an enhancement of the effect for the tracks crossing the transition region as compared to tracks located in the EC region only. As a result, one could recognize possible EC-sector rotations by the relative increase of the Z width using tracks crossing different regions of the EC detector.

Furthermore, misalignments stemming from the EC-sector rotations around a transverse axis produce recognizable phi effects as well. In fig.14, the slope of the Z width increase is plotted for different phi sectors. The distribution, despite the small statistics, which is reflected by the big statistical errors, follows the pattern expected for a rotation around the x axis.

Obviously, the width of the Z can be affected by a number of other factors, as well. However, the sort of misalignments discussed here, can have some unique influence on the mass scale and on the Z resolution, which can be spotted very easily and create the basis of further detailed studies involving straight track residuals in the barrel/EC region etc.

4. CONCLUSIONS

An algorithm was developed to perform a constrainted fit on the di-muon effective mass using a Breit-Wigner mass distribution approach for the Z mass. If the muon spectrometer stand-alone reconstruction is only taken into account, then this method permits a decrease of the background of the order of 20% for a SM Higgs of 200 GeV/c^2.

Projective misalignments at the level allowed by the predicted accuracy of the alignment system will not affect SM Higgs reconstruction of masses in the region of 200 to 300 GeV/c^2. On the contrary, EC-sector translations (or rotations) affect the reconstructed Higgs width (this applies to the scenario of constraining the di-muon masses to a BW Z mass, as well). However, "moderate" values of misalignment (translations or rotations), do not seem to affect the acceptance of Higgs events in a "reasonably" wide (2σ) mass window, with the exception of large rotations around axes perpendicular to the beam, where a significant inefficiency in the muon reconstruction is observed. However, these particular rotations, which are NOT global EC-rotations, will be detected by the forward alignment system (if they exceed a few hundreds microrads).

In addition, given the fact that we shall have large statistics of Z bosons, we can use the sample to recognize possible misalignments and to correct for them, even if the misalignments are smaller than the ones treated here.

In the future, we would like to use the full detector simulation to perform a similar study in order to:

a) Study the effect of muon spectrometer misalignment using the combined MUON-ID information
b) Study the effect of possible misalignments between the muon spectrometer and inner detector
c) Use in addition the tile calorimeter information to correct for the energy loss of the muons.
d) Include noise effects, pileup events and Drell-Yan background in the simulation procedure.

Finally we would like to investigate the effect of misalignment on the reconstruction of SUSY Higgs -> 2 μ, where the mass constraint cannot be applied, and on the SM Higgs -> ZZ*, where the mass constraint can only be applied to one Z.

REFERENCES

1. Atlas Muon Collaboration, 'ATLAS Muon Spectrometer TDR', **CERN/LHCC/97-22**
2. L.Chevalier, 'LHCTOR: A stand alone Geant Program for simulation of the ATLAS spectrometer'**, ATL-MUON-97-147**
3. M.Virchaux et al.**, '**Muonbox: a full 3D tracking program for Muon reconstruction in the ATLAS Spectrometer', **ATL-MUON-97-198**
4. *http://atlas.web.cern.ch/Atlas/GROUPS/PHYSISCS/MUON/muid.html*
5. Avolio, G., Cerutti, F., **'**On the impact of the muon spectrometer alignment on the search for the SM Higgs boson in the 4mu channel'**, ATL-MUON-2001-001**
6. *http://atlas.web.cern.ch/Atlas/GROUPS/MUON/AMDB_SIMREC/amdb_simrec.html*

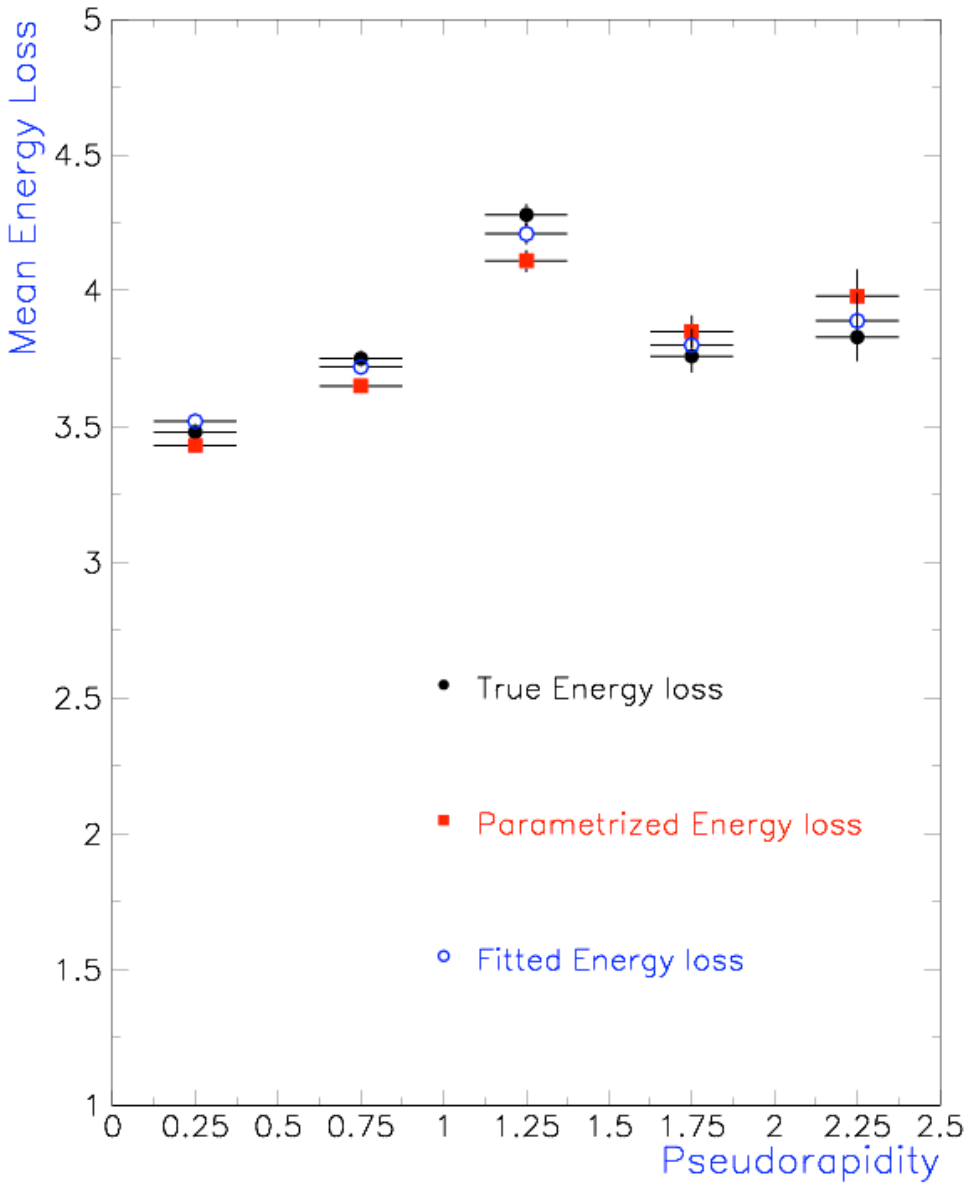

Figure 1: Energy loss of muons of momenta $30< p <70$ GeV/c as a function of η. The squares are the energy loss estimation from the parametrization described in the text, the full circles are the actual energy loss obtained from the MC and the open circles the energy loss estimated after the constrained fit.

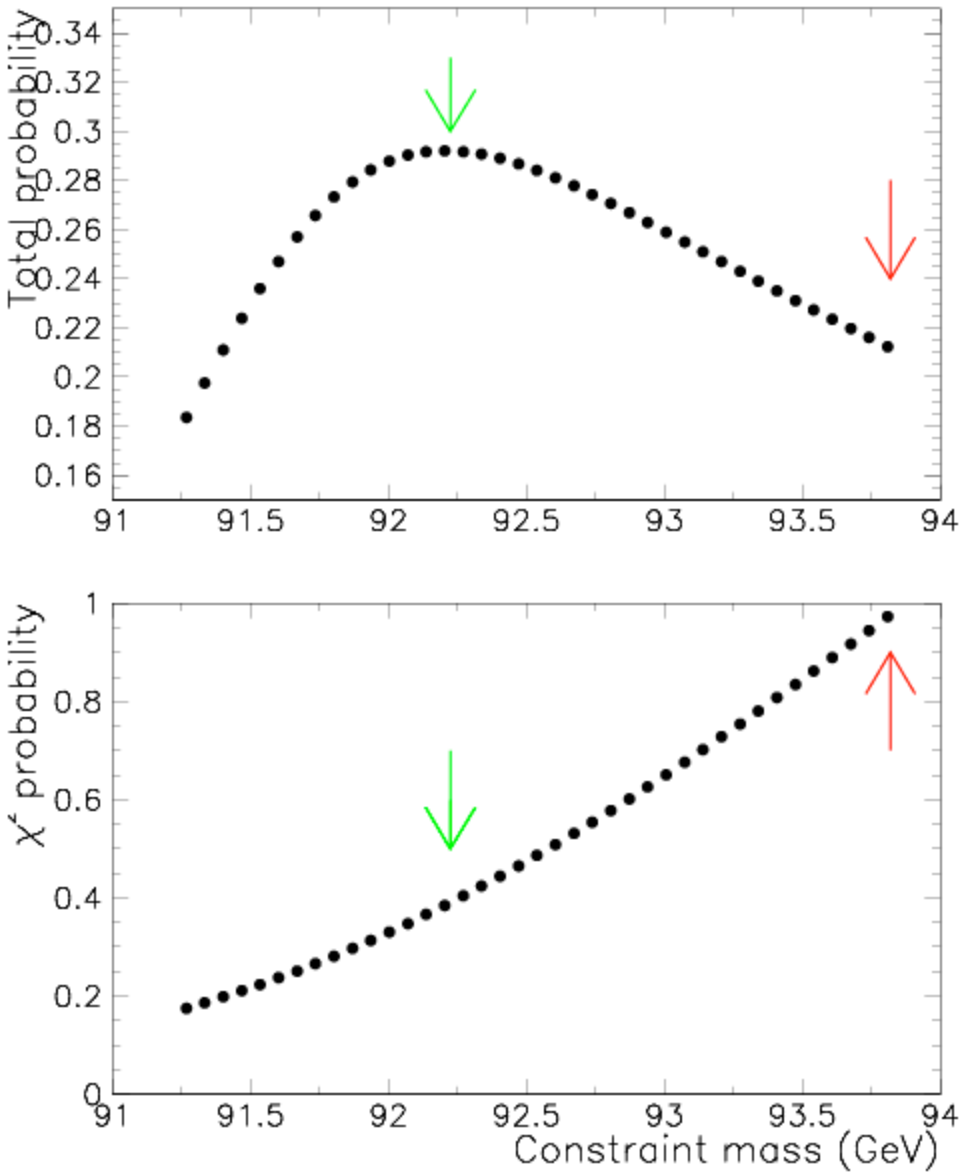

Figure 2 a) and b) show the probability and the $\chi 2$ respectively as a function of the di-muon mass for a typical event. With green arrow we indicate the initial unfit mass value and with red arrow, the fit value.

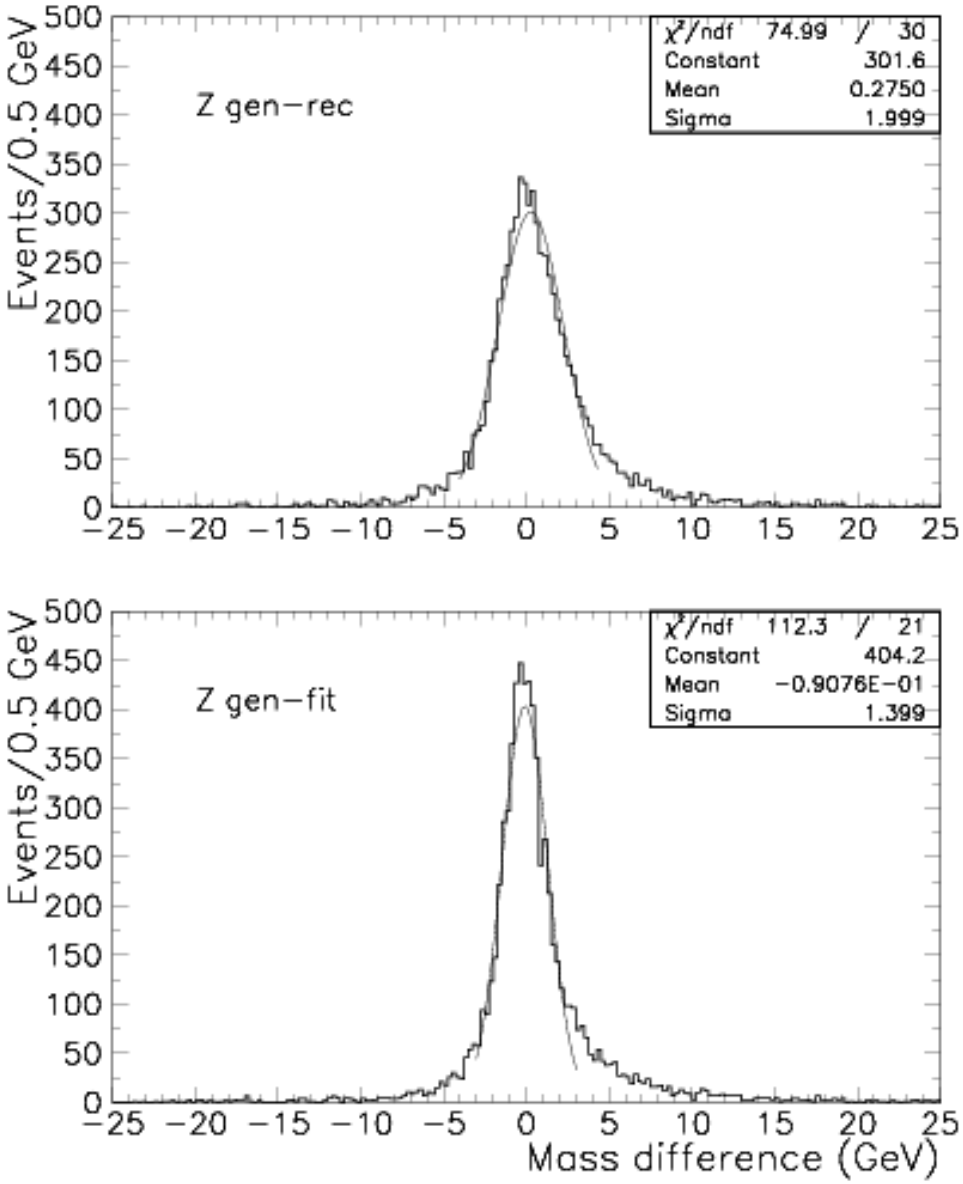

Figure 3: The reconstructed minus the generated di-muon mass from 200 GeV/c^2 Higgs decays, before and after the constrained fit described in the text

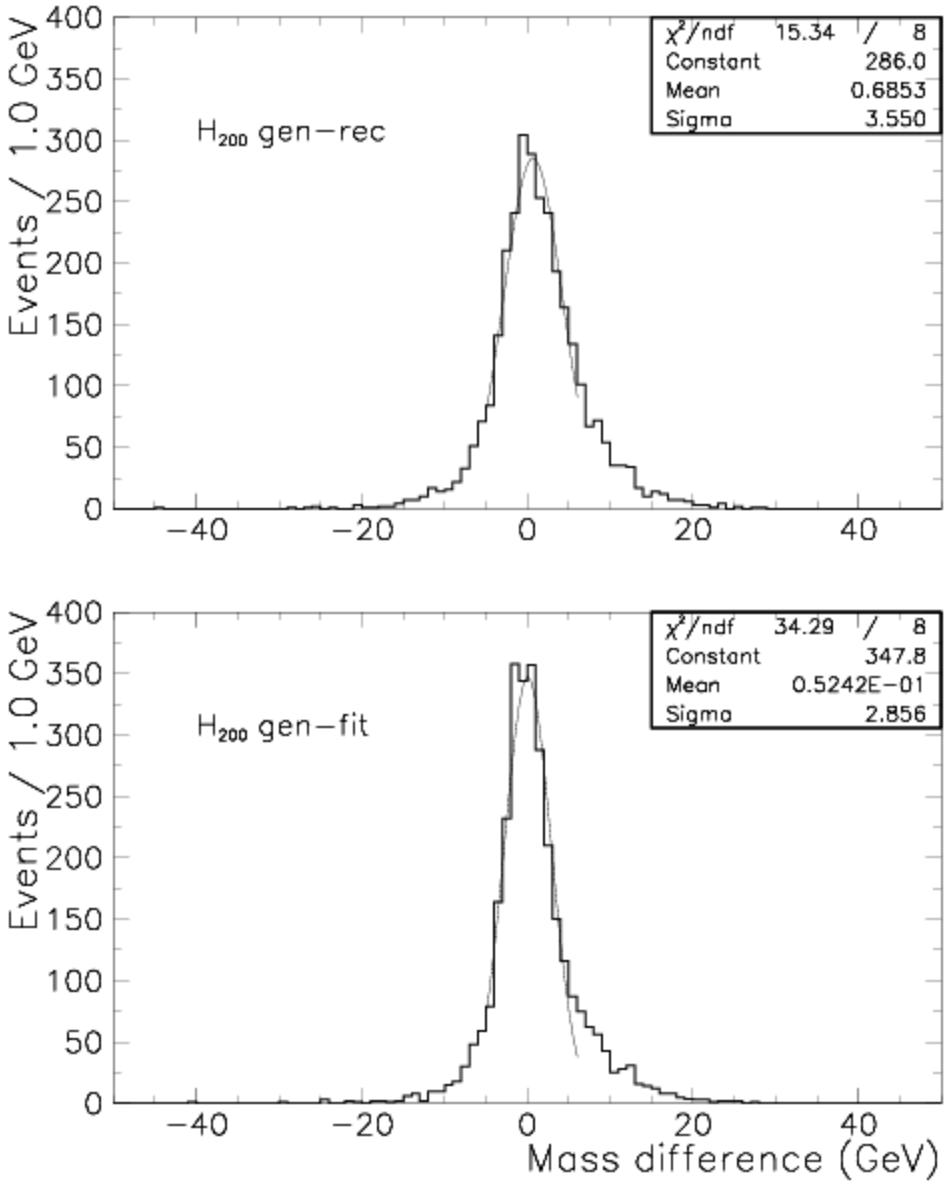

Figure 4: shows the reconstructed minus the generated Higgs mass before and after the constrained fit described in the text. The generated Higgs had a 200 GeV/c^2 mass.

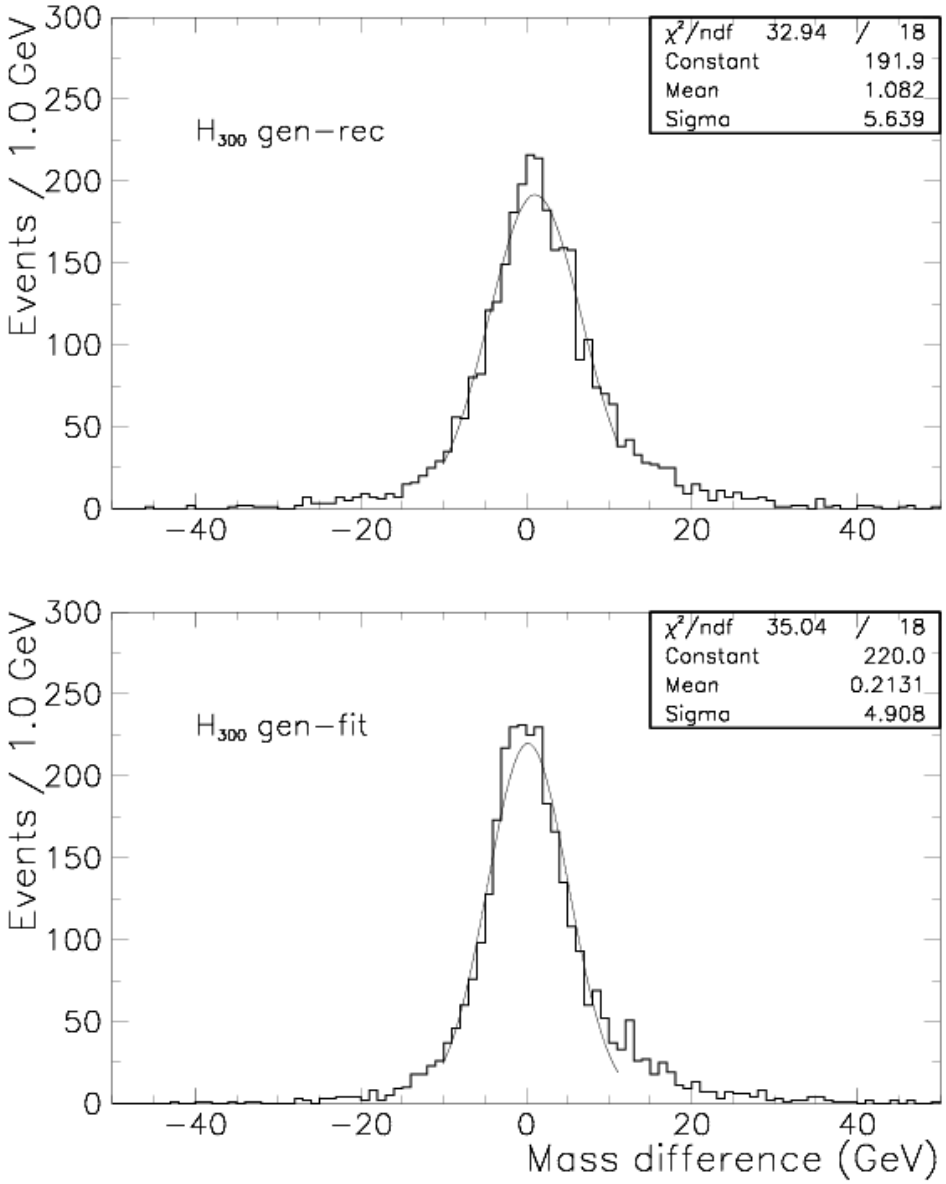

Figure 5: shows the reconstructed minus the generated Higgs mass before and after the constrained fit described in the text. The generated Higgs had a 300 GeV/c^2 mass.

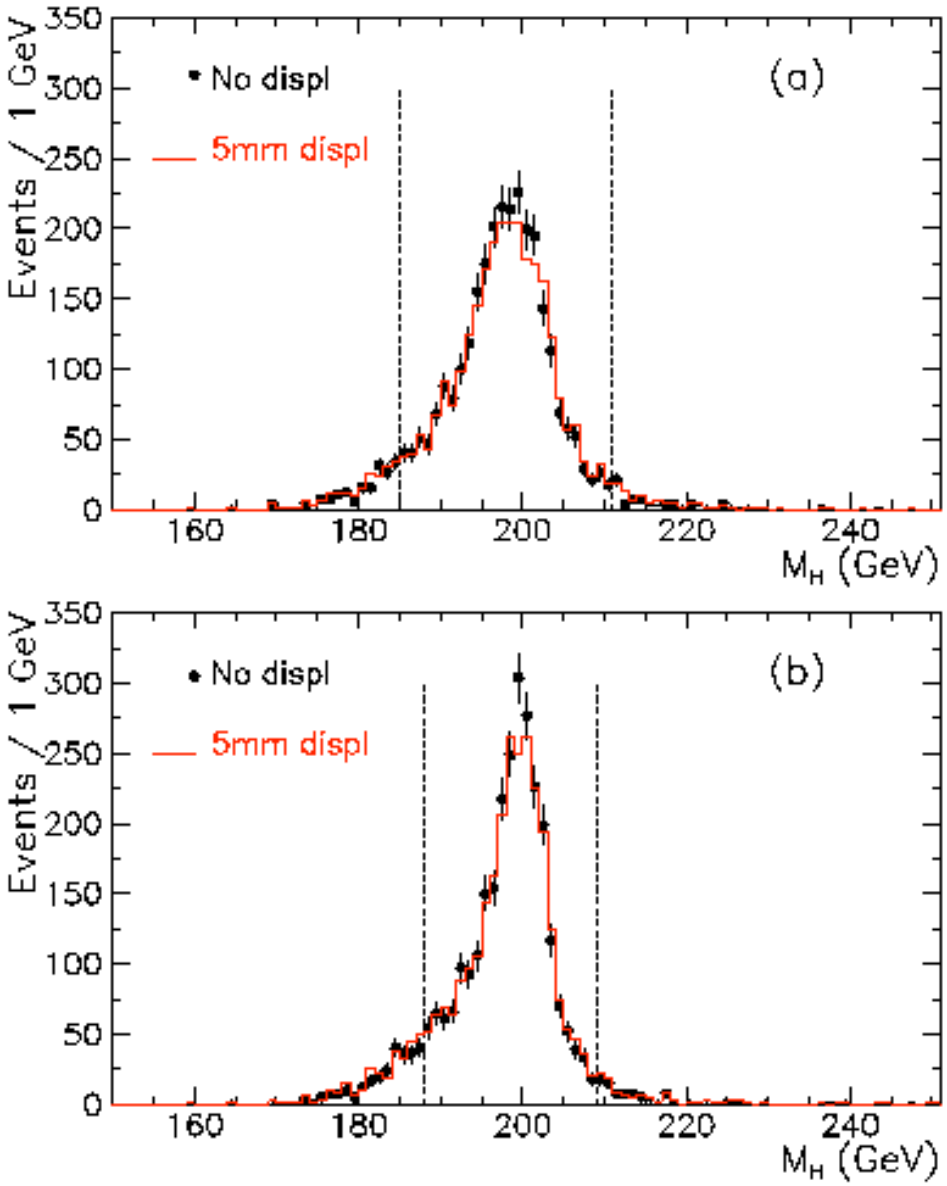

Figure 6: The effect of 5 mm longitudinal displacement of one EC on the reconstructed **200 GeV/c^2 Higgs** mass **(a),** and on the fitted one using a Breit-Wigner *Z* mass constraint **(b)**. The lines indicate the mass windows used in each case.

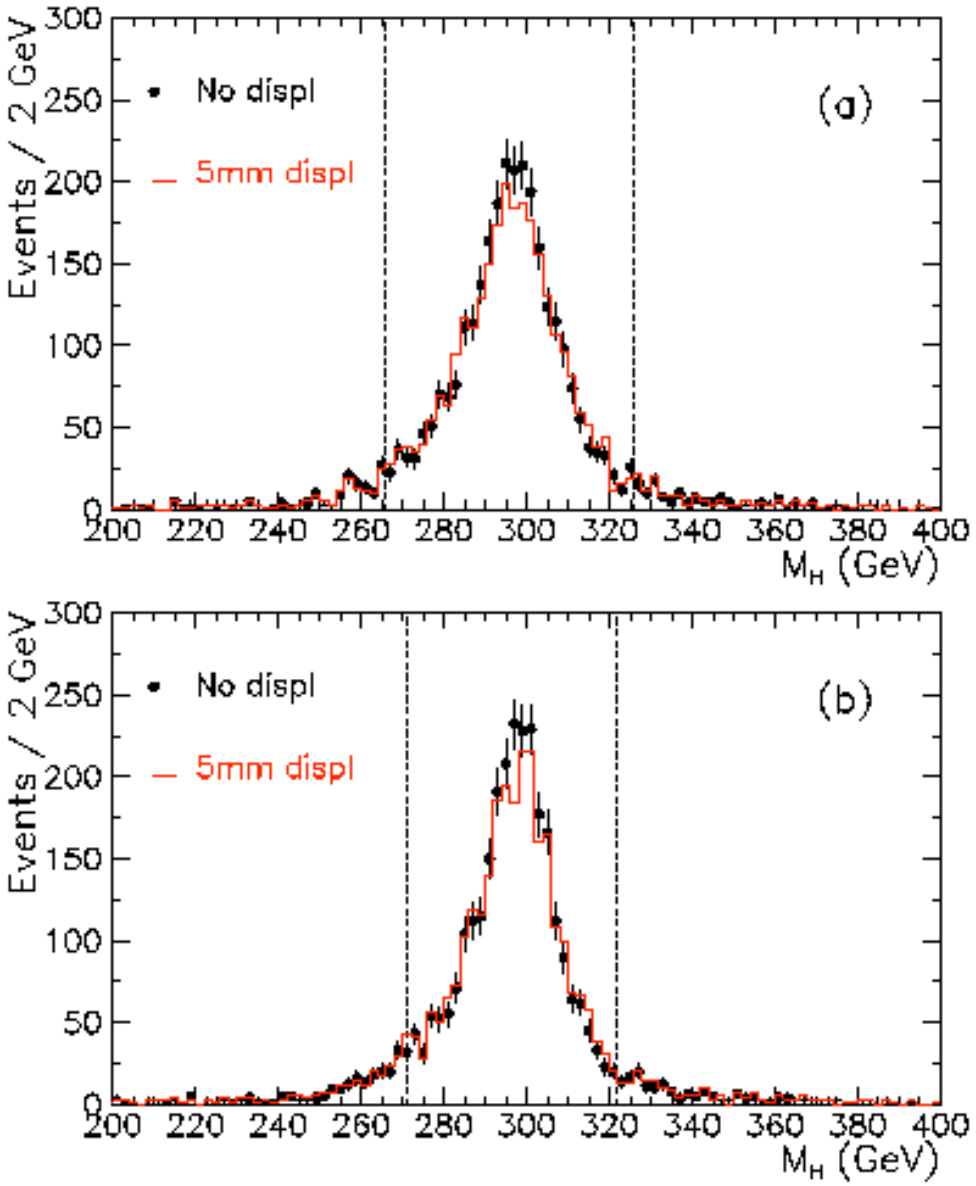

Figure 7: The effect of 5 mm longitudinal displacement of one EC on the reconstructed **300 GeV/c^2 Higgs** mass **(a),** and on the fitted one using a Breit-Wigner *Z* mass constraint **(b)**. The lines indicate the mass windows used in each case.

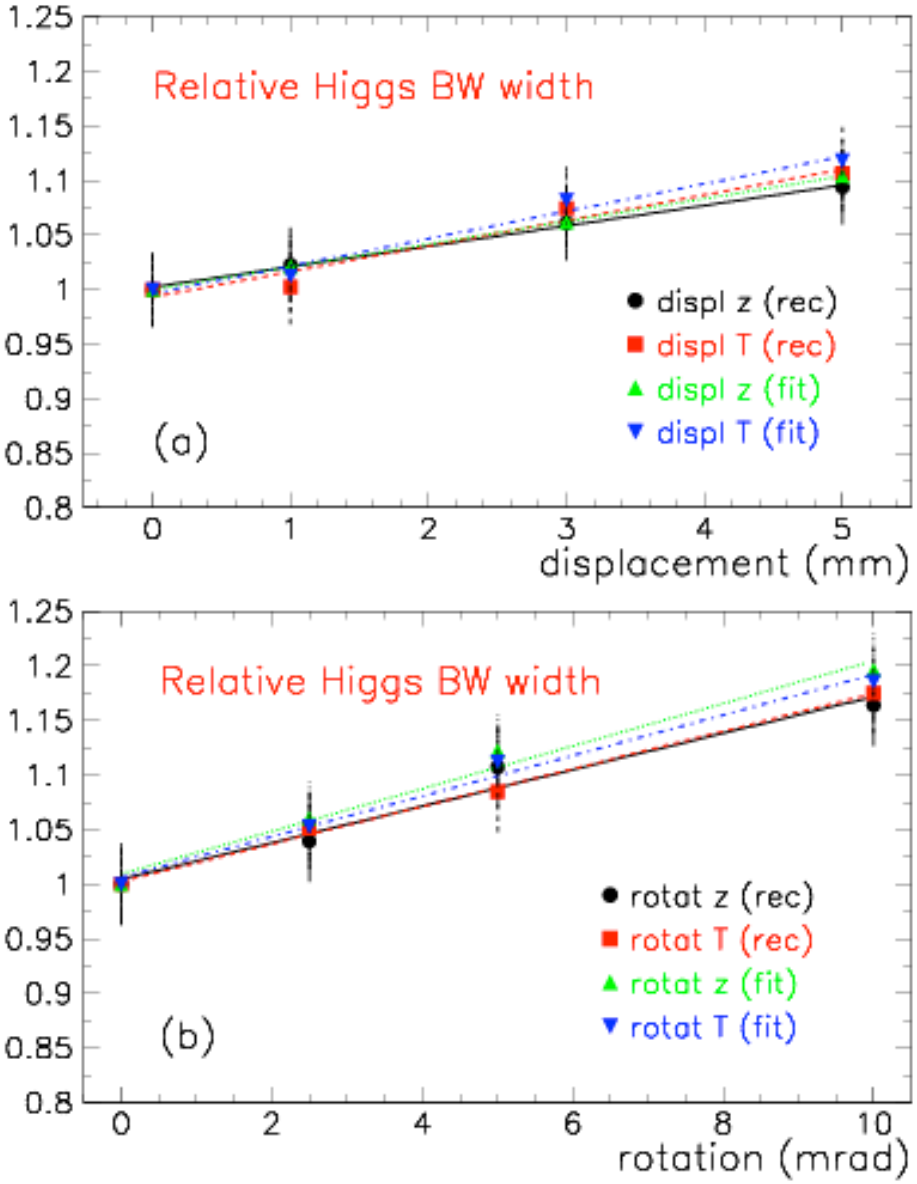

Figure 8: The relative increase of the width of the reconstructed or fitted **200 GeV/c^2 Higgs** as a function of the size and type of translation **(a)** and rotation **(b)**. The lines correspond to linear fits showing the trend of the increase.

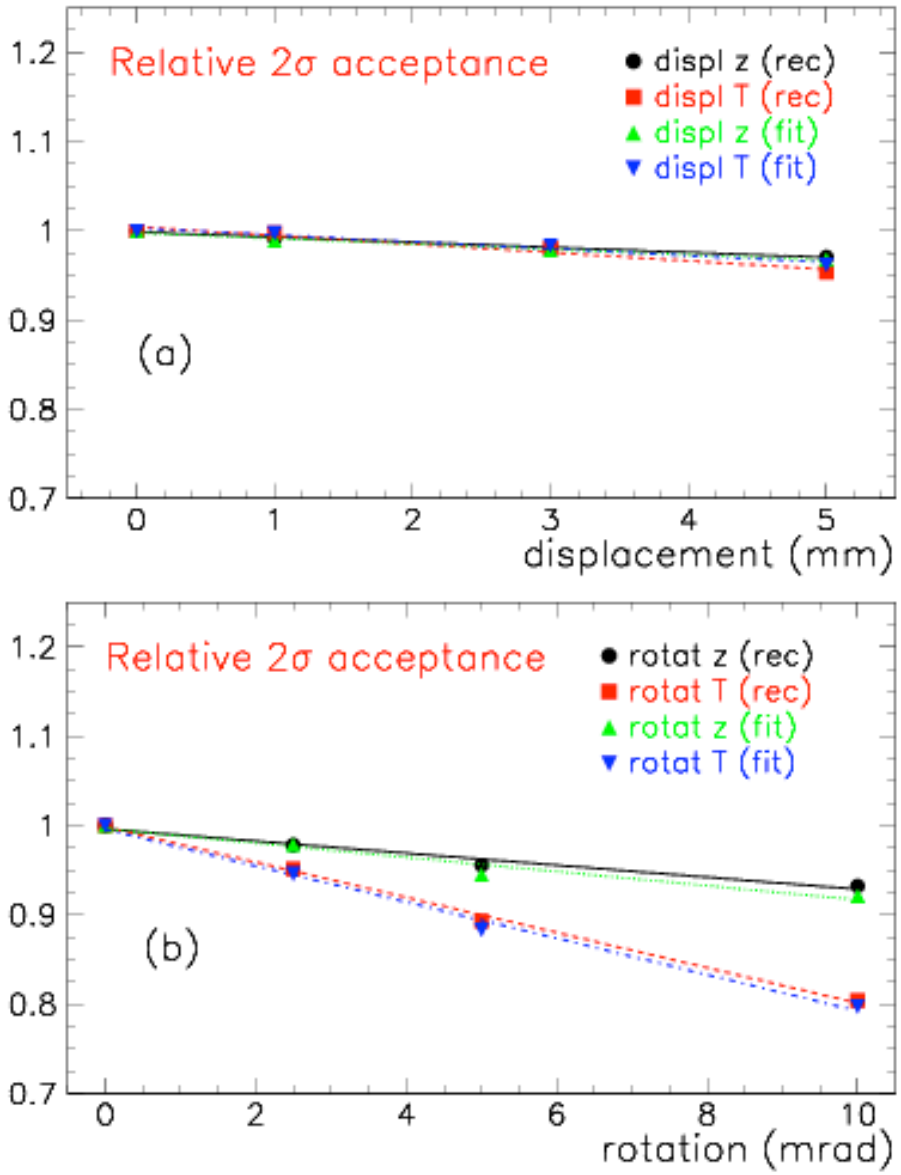

Figure 9: The relative decrease of the number of accepted, reconstructed or fitted **200 GeV/c^2 Higgs** as a function of the size and type of translation **(a)** and rotation **(b)**. The lines correspond to linear fits showing the trend of the decrease.

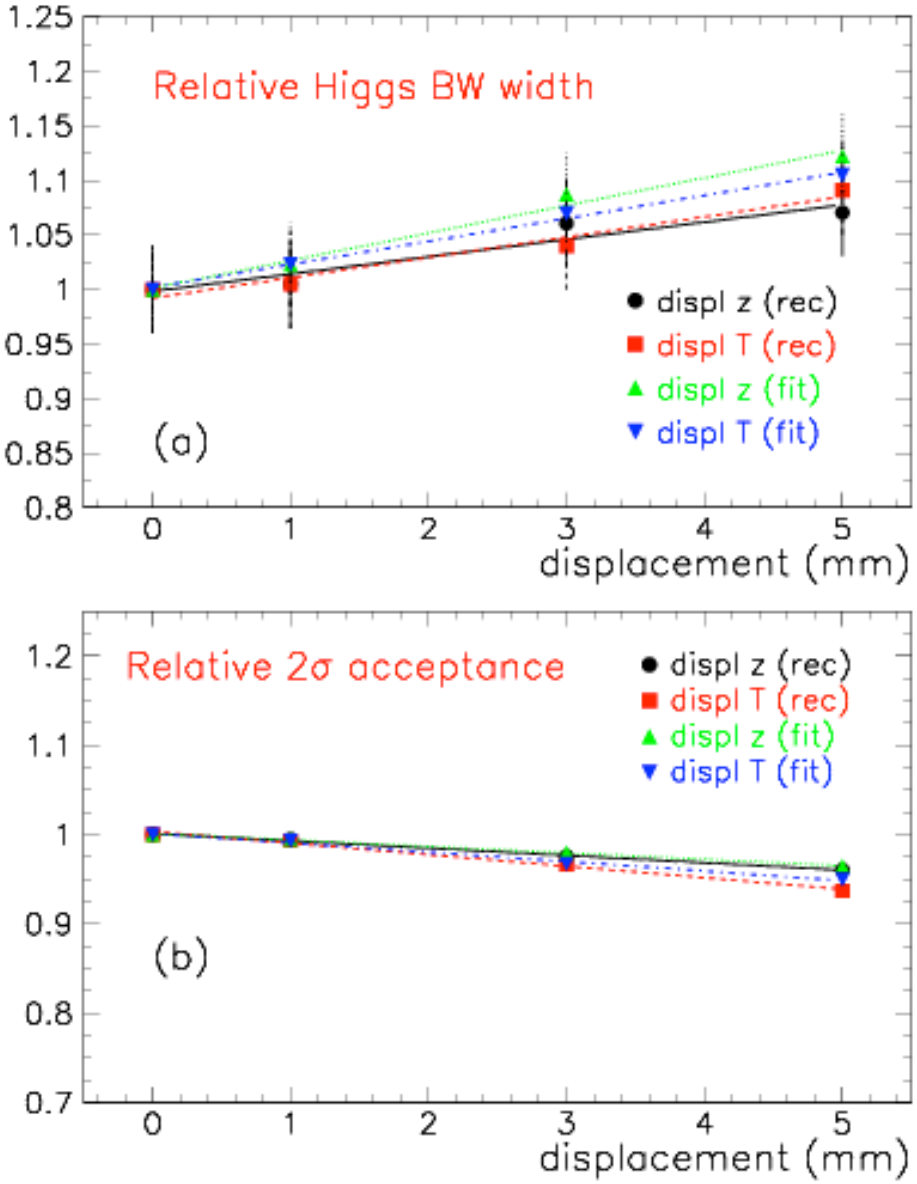

Figure 10: The relative increase of the width **(a)** and decrease of the accepted number **(b),** of reconstructed or fitted **300 GeV/c^2 Higgs** as a function of the size and type of translation The lines indicate the mass windows used in each case. The lines correspond to linear fits showing the general trend.

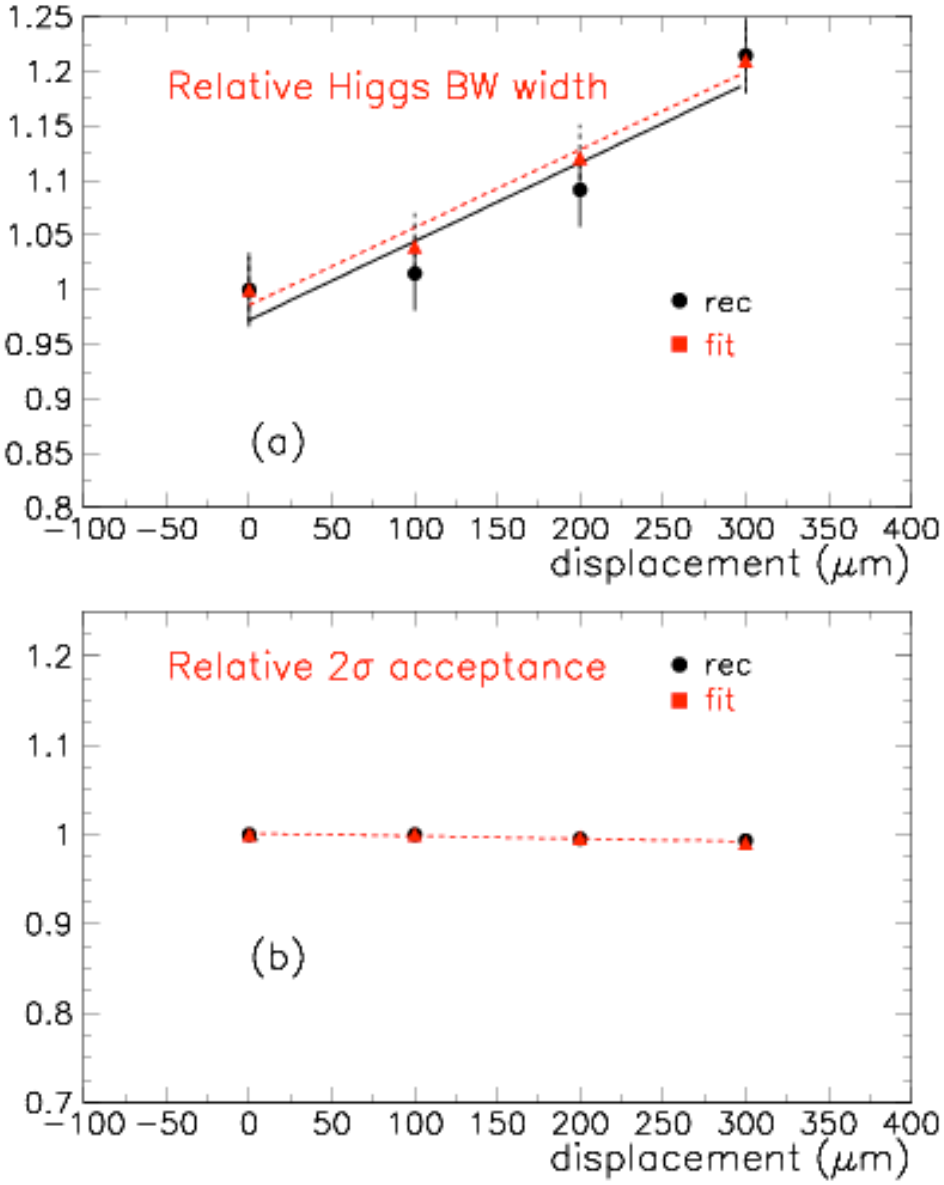

Figure 11: The relative increase of the width **(a)** and decrease in the number of accepted **(b),** reconstructed or fitted **200 GeV/c^2 Higgs** as a function of the size of the systematic translation of all the muon middle stations (both barrel and EC) in the way discussed in the text.

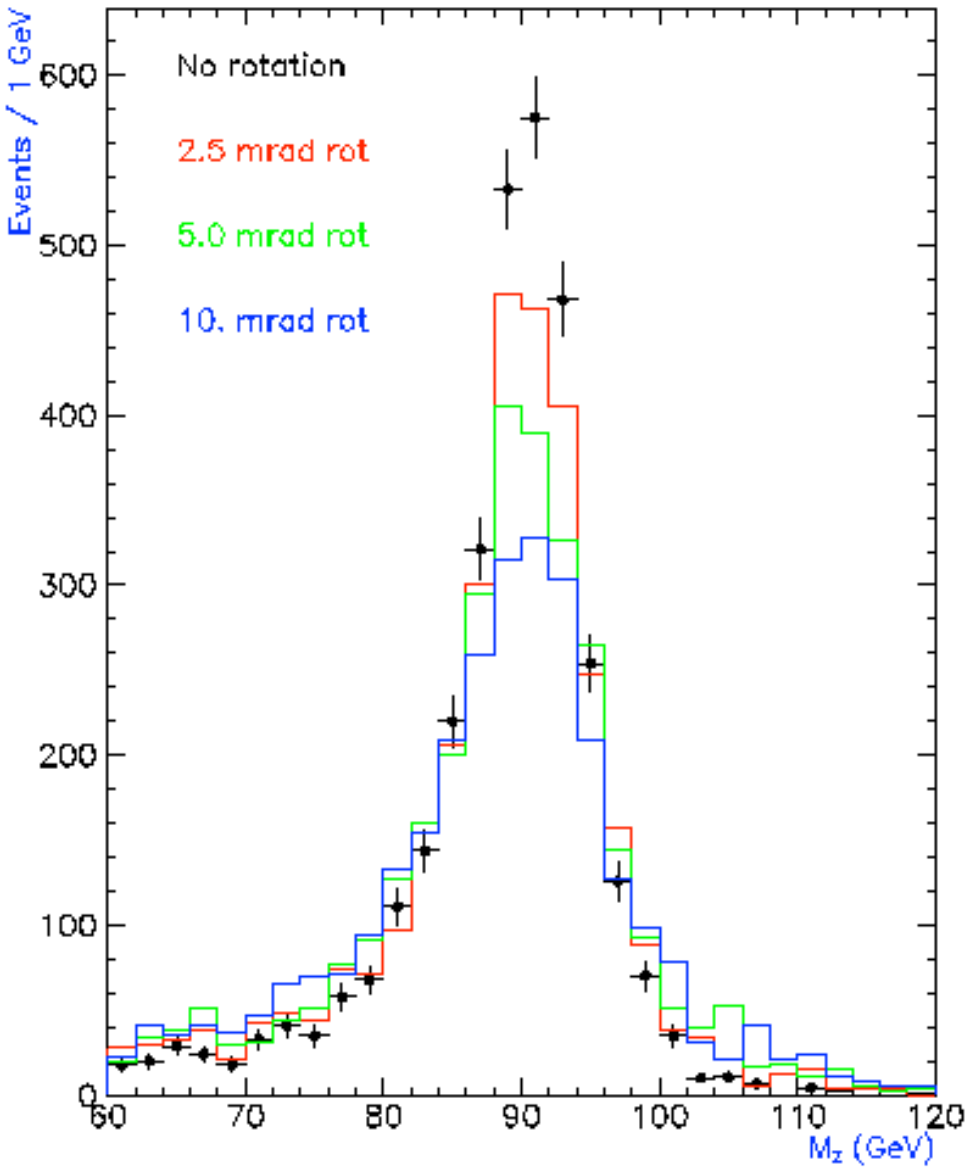

Figure 12: The effect of 2.5, 5 and 10 mrad rotation- of all sectors belonging to one EC, around the ATLAS x- axis- on the reconstructed **Z** mass.

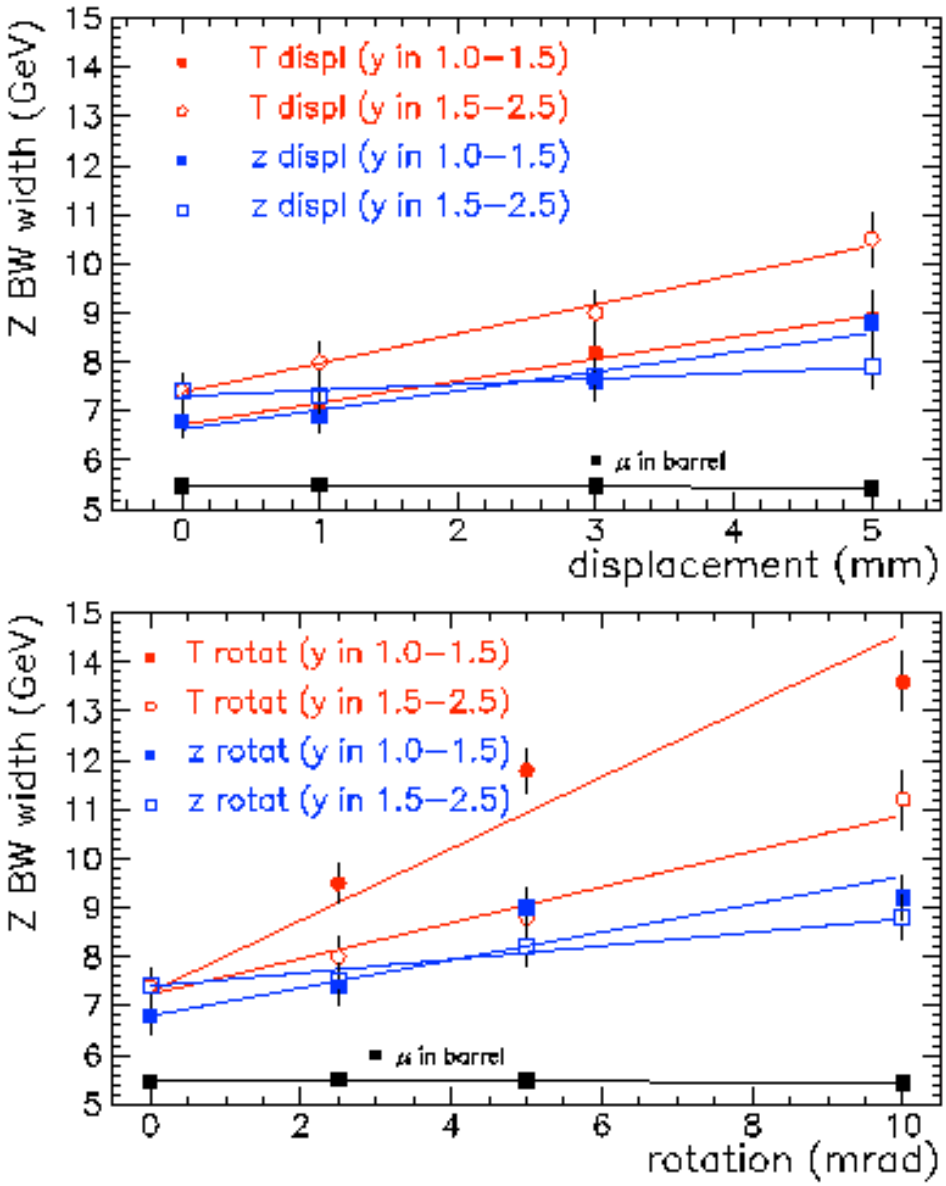

Figure 13: The relative increase of the width of the reconstructed **Z mass** as a function of the size and type of translation **(a)** and rotation **(b)**. The lines correspond to linear fits showing the trend of the increase. At least one muon was required to be reconstructed in the misaligned area. The case where both muons are in the barrel is also shown for comparison.

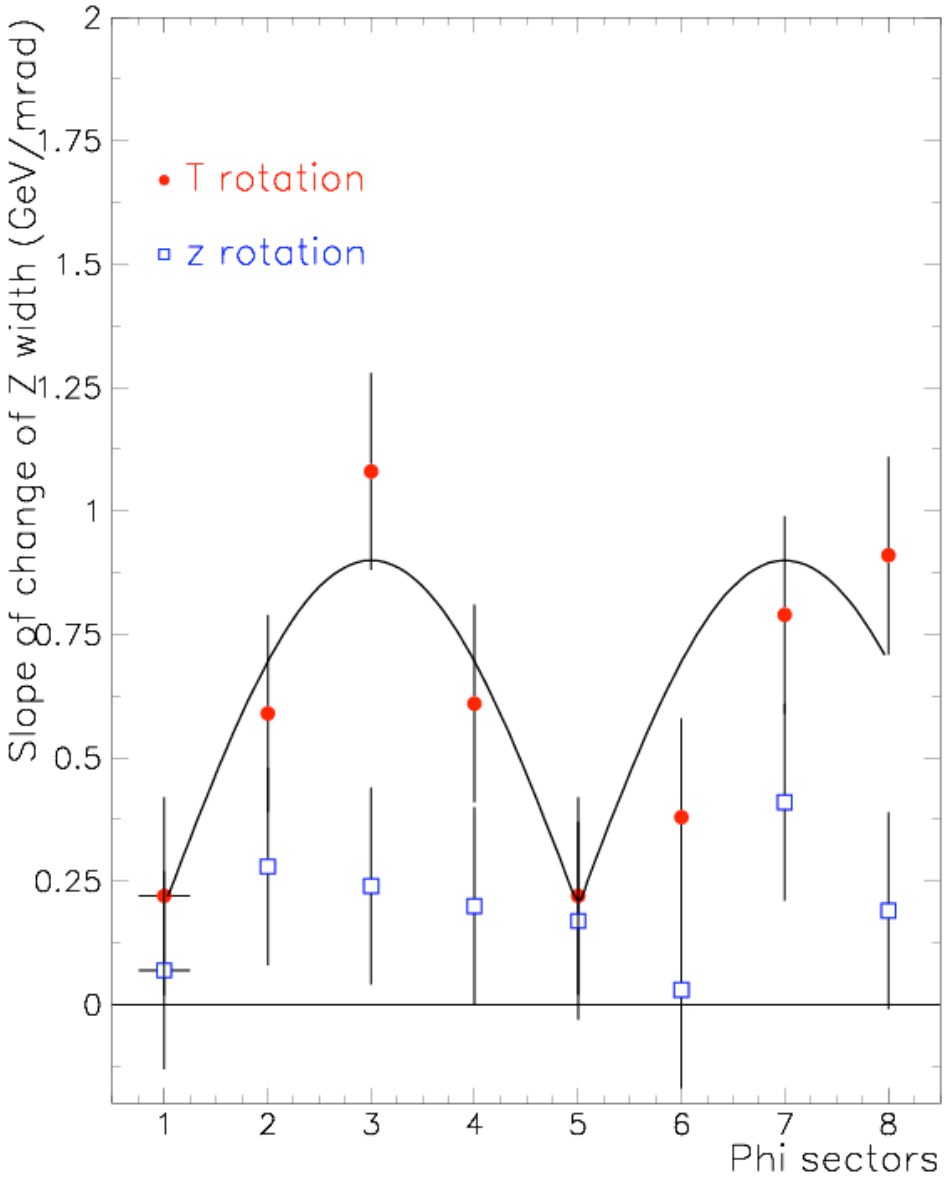

Figure 14: The modulation of the slope of the increase of the width of the reconstructed **Z mass** as a function of phi, for rotations around the x axis (red circles) and the z axis (blue rectangles).